Acta Oceanol. Sin., 2019, Vol. 38, No. 1, P. 90–101
https://doi.org/10.1007/s13131-019-1374-x
http://www.hyxb.org.cn
E-mail: hyxbe@263.net

A model for the transportation and distribution of jellyfish *Rhopilema esculentum* for stock enhancement in the Liaodong Bay, China

Liping Yin[1, 2, 3], Xiujuan Shan[4, 5], Chang Zhao[1, 2, 3, 6], Xianshi Jin[4, 5], Guansuo Wang[1, 2, 3], Fangli Qiao[1, 2, 3*]

[1] First Institute of Oceanography, Ministry of Natural Resources, Qingdao 266061, China

[2] Laboratory for Regional Oceanography and Numerical Modeling, Pilot National Laboratory for Marine Science and Technology (Qingdao), Qingdao 266237, China

[3] Key Laboratory of Marine Science and Numerical Modelling, Ministry of Natural Resources, Qingdao 266061, China

[4] Yellow Sea Fisheries Research Institute, Chinese Academy of Fishery Sciences, Qingdao 266071, China

[5] Laboratory for Marine Fisheries Science and Food Production Processes, Pilot Qingdao National Laboratory for Marine Science and Technology (Qingdao), Qingdao 266237, China

[6] Key Laboratory of Data Analysis and Applications, Ministry of Natural Resources, Qingdao 266061, China

Received 6 January 2018; accepted 22 March 2018

Abstract

A numerical model for jellyfish *Rhopilema esculentum* stock enhancement is developed for the first time. The model is based on an operational ocean circulation-surface wave coupled forecasting system for the seas off China and adjacent areas and uses a Lagrangian particle-tracking scheme to track the trajectories of released jellyfish. The Jellyfish are modeled as particles with diel vertical migration and are passively drifted by the current and dispersion due to the sub-grid processes. A comparison between the simulation and survey results demonstrate that the model can capture the primary distribution patterns of the released jellyfish. The model results show that the ocean current and indirect wind impact are the main drivers controlling the jellyfish transport. A connectivity matrix between the release sites and fishing grounds indicates the top of the bay is better than the eastern and western coasts for jellyfish fishing. The matrix also shows that only 45% and 27% of the jellyfish released from Wafangdian (WFD) can enter the fishing ground in 2008 and 2010; thus, the site near WFD is not an advisable location for jellyfish release. A Lagrangian probability density function based on a nine-year tracing experiment validates the results and further provides a "climatology" distribution of the released jellyfish. Several experiments are conducted to examine the sensitivity of the model to random walk schemes and to release conditions. The model requires a random walk but is insensitive to the random walk scheme. The experiments with different habitat depths show that if the jellyfish are fixed on the bottom of the water, most of them will be transported to the center, or even out of the bay, by the bottom circulation.

Key words: Liaodong Bay, Jellyfish *Rhopilema esculentum*, distribution and connectivity, Lagrangian particle tracking, current

Citation: Yin Liping , Shan Xiujuan , Zhao Chang , Jin Xianshi , Wang Guansuo , Qiao Fangli . 2019. A model for the transportation and distribution of jellyfish *Rhopilema esculentum* for stock enhancement in the Liaodong Bay, China. Acta Oceanologica Sinica, 38(1): 90–101, doi: 10.1007/s13131-019-1374-x

1 Introduction

The jellyfish *Rhopilema esculentum* is most commonly observed in China and Southeast Asia (Omori and Nakano, 2001). This species is a traditional and popular seafood, and has a high medicinal value (You et al., 2007). In recent years, the market for jellyfish has increased. Correspondingly, jellyfish capture, production, and processing have increased in several countries (Pitt and Kingsford, 2003). In China, the jellyfish widely distributed off the Chinese coast. Especially in the Liaodong Bay (LDB), the jellyfish is one of the most economically important species, and fishermen's incomes are significantly affected by the availability of it.

Because of a sharp decline in jellyfish resources, restocking and stock enhancement research has been implemented regularly since the 1980s in Liaoning, Zhejiang and Shandong Provinces, China (Jin, 2014). Jellyfish stock enhancement was

Foundation item: The National Natural Science Foundation of China under contract No. 41506044; the Scientific and Technological Innovation Project financially supported by Qingdao National Laboratory for Marine Science and Technology of China under contract No. 2016ASKJ02; the National Basic Research Program (973 Program) of China under contract No. 2015CB453303; the National Natural Science Foundation of China-Shandong Joint Fund for Marine Science Research Centers under contract No. U1606405; the International Cooperation Project of Indo-Pacific Ocean Environment Variation and Air-Sea Interaction under contract No. GASI-03-IPOVAI-05.

*Corresponding author, E-mail: qiaofl@fio.org.cn

first conducted in Liaoning Province from 1984 to 2004, where 11 restocking experiments were carried out (Dong et al., 2009). Productive stock enhancement has been implemented in the LDB since 2005. This artificial stock enhancement has effectively increased the jellyfish yield.

Rhopilema esculentum is planktonic throughout its life with weak swimming ability. It can only swim forward at speeds of 0.06–0.08 m/s in static water (Li et al., 2008). Similar to many zooplanktons, the jellyfish has a sensitive sensory system and exhibits diel vertical migration (DVM). It migrates to the bottom or near-bottom of its habitat at night or in adverse conditions such as strong wind, heavy rain, or rapid flow. In the daytime, it migrates to the surface of the sea (Dong et al., 2013).

The distributions of jellyfish are related to its ecological characteristics (Dong et al., 2009). However, surface wind direction and speed, ocean current and tide also influence its distributions (Jin, 2014) through transport processes. In the LDB, the jellyfish is geographically independent and remains in the bay throughout its life cycle.

In June, the jellyfish inhabits shallow coastal waters within the 5 m isobaths. Some of the jellyfish move to deeper waters during July. However, approximately 90% of the jellyfish in the LDB remain within the 5 m isobaths north of 40°30′N (Jin, 2014). The jellyfish drift passively with the horizontal currents. Therefore, to understand their distribution and the connections between release and catch areas, we must consider jellyfish transport by the ocean currents and other physical processes in the LDB.

The LDB is dominated by a regular semidiurnal tide. The strongest tidal current (approximately 0.6 m/s) appears near the Changxing Island on the western coast and Suizhong County on the eastern coast (Xiong, 2012). Tides induce residual currents because of terrain changes within the bay. The Lagrangian residual current is dominated by the prevailing wind. The water depth in the LDB is shallow, varying from no more than 5 m on the coast to 30 m at the bay center (Fig. 1). This shallowness enables the bottom friction to exert a notable influence on the current, and the residual currents change significantly from the surface to the bottom of the LDB. On the surface, the direction of the residual currents is similar to that of the wind; a clockwise circulation presents on the bottom during the summer (Zhao et al., 1995; Qiao, 2012; Xiong, 2012). The speed of the bottom residual current is no more than 0.03 m/s, except at the top of the bay and the bay mouth where the speed may exceed 0.05 m/s (Jiang et al., 2002).

The variations of the annual circulation may result in different jellyfish distributions and affect the jellyfish yield. The development of high-resolution ocean circulation models enables the temporal and spatial variability of ocean currents and other physical factors to be simulated and forecasted. Based on this, a Lagrangian particle tracking method or an individual-based model (Grimm, 1999) are the efficient ways to understand the spatiotemporal-dependent transport of particles driven by the ocean currents. This method has been successfully applied to harmful jellyfish transport from strobilation source zones to regions of interest (Moon et al., 2010; Berline et al., 2013).

In this study, we will use the particle-tracking experiments based on a three-dimensional ocean circulation model to study the factors that affect the spatio-temporal variations of the jellyfish distribution and the connectivity between the release areas and the fishing grounds in the LDB. It is efficient and necessary to use a numerical model to research the physical impacts on the fishery stock enhancement and releasing. However, we have not found study about this in China up to now. This study may supply fundamental scientific insight to the stock enhancement and management for jellyfish and other ocean species.

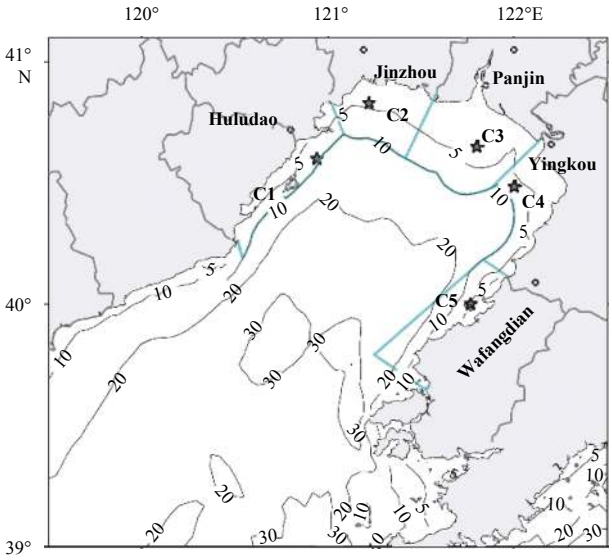

Fig. 1. The map of the LDB. The stars represent the release sites of young jellyfish from Dong et al. (2009). The contours are the 5, 10, 20 and 30 m isobaths. The traditional fishing ground from Dong et al. (2009) is divided into five parts by the administrative divisions (cyan polygons C1 through C5). The polygons are the analysis grids, representing the connectivity between the release and capture areas on the basis of the model results.

2 Methods

2.1 *Ocean circulation model*

The ocean circulation-surface wave coupled forecasting system (OFS-C) was developed for the seas off China and adjacent areas (15°–41°N, 105°–135°E). The operation starts at 12:00 UTC daily and provides 72 h oceanic forecasting products, including tide, current, temperature, salinity, sea level and significant wave height. The OFS-C is based on the synchronous coupling of the Princeton Ocean circulation Model (POM) and Key Laboratory of Marine Science and Numerical Modeling (MASNUM) surface wave model (Yuan et al., 1991; Yang et al., 2005). The MASNUM provides the wave-induced mixing parameter (Bv) and then transferred to the circulation model (Qiao et al., 2004a, b), leading to an improvement of the upper ocean simulation. The circulation and wave models are parallelized using message-passing interface techniques to reduce their runtimes. The circulation model contains 30 vertical sigma layers and 721×625 horizontal grid points, with a horizontal resolution of (1/24)°×(1/24)°. A triple-nested technique is used to generate lateral boundary conditions (temperature, salinity, sea level and velocities): a (1/8)°×(1/8)° northwestern Pacific model (0°–50°N, 99°–150°E) (Xia et al., 2004b) and a (1/2)°×(1/2)° global model (Xia et al., 2004a), which provides the lateral boundary conditions for the northwestern Pacific model. The surface boundary condition for the surface momentum and heat fluxes is provided by a global spectral data assimilation and forecast model system (GFS) (for the global model) and a regional meteorological forecast model (MM5) (for the regional model). For every day of the forecast run, a hot restart is implemented by assimilating the high-resolution SST into the system via a modified nudging method. The SST is derived from the North-East Asian regional project of the global

ocean observing system (NEAR-GOOS) (Wang et al., 2016).

The comparisons between the observations and forecasting results have demonstrated the reliability and validity of this ocean forecasting system (Wang et al., 2016). The forecasting system accurately reproduces the current in the LDB. Figure 2 shows the monthly mean current and sea surface wind fields in the LDB during the summer (June to August) simulated by the OFS-C. The surface monthly mean current (Figs 2a–c) is strongly affected by the wind (Figs 2g–i). The currents on the sea surface differ significantly from those on the bottom when the wind is strong. During these periods, the speeds of the currents on the surface are higher than 0.05 m/s, and their direction is similar to that of the wind; on the bottom, the speeds are lower than 0.03 m/s, and the currents form a clockwise cycle. In August, the wind weakens, and the currents on the surface and bottom of the LDB are similar. The modeled bottom current is similar to the observed current, exhibiting relatively higher speeds in shallow waters and lower speeds in deep waters (Jiang et al., 2002).

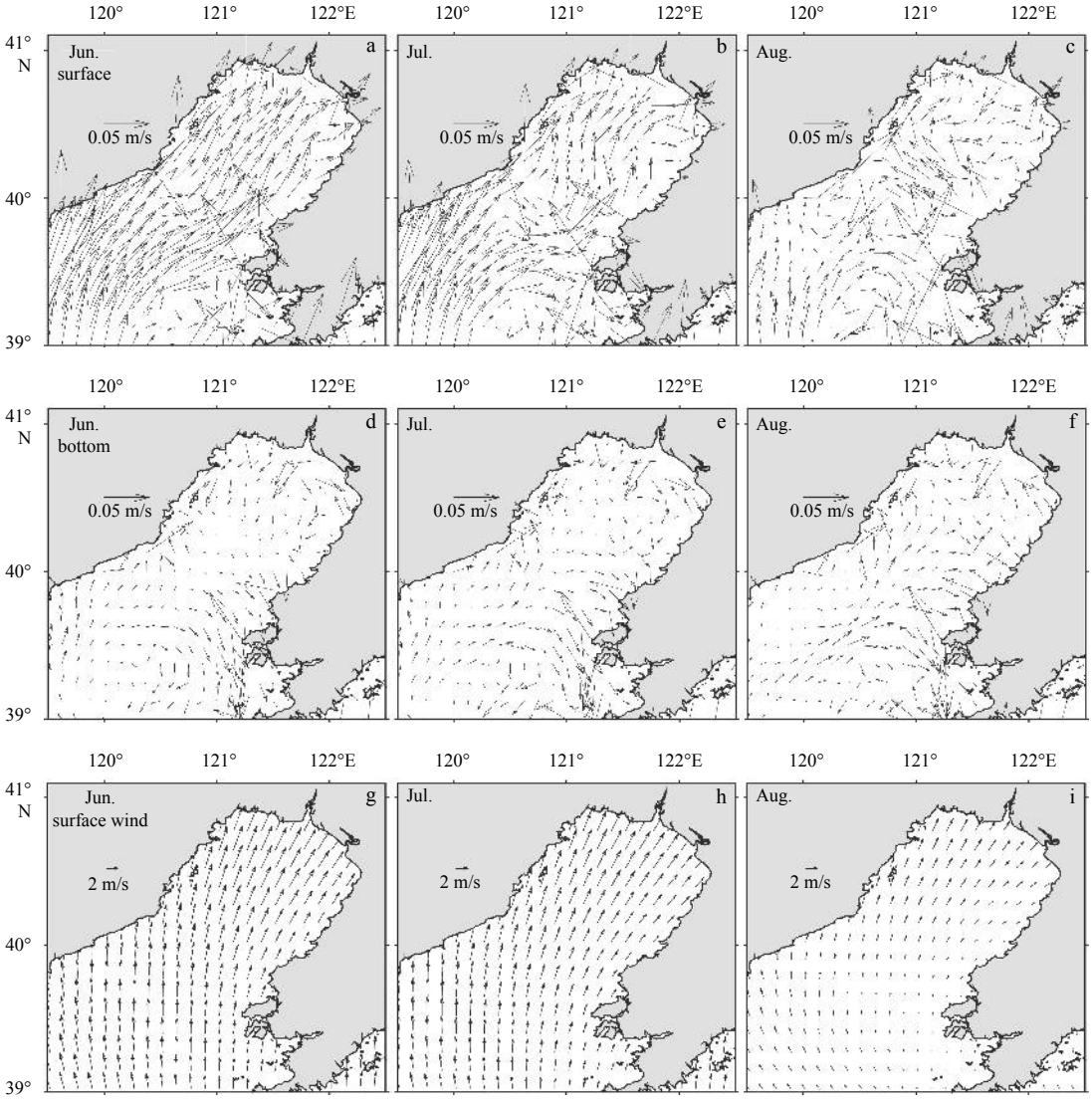

Fig. 2. Three-year (2008–2010) monthly averaged surface (a, b and c) and bottom layer (d, e and f) current fields for June to August and the wind fields for the same period (g, h and i). Data are derived from OFS-C.

In this study, the OFS-C output was extracted (39°–41°N, 119.5°–122.5°E) and used to track the jellyfish transport from release to harvest. The grid configuration within the tracking domain comprised of 166×120 horizontal spatial points and 30 vertical sigma layers from the surface to the bottom. Three-dimensional velocity data were output every 3 h from the OFS-C simulation. As the transport time of the jellyfish we focused is about 2 months, the temporal resolution of the model output is sufficient.

2.2 *Lagrangian particle tracking method*

The Lagrangian particle tracking method was used to track the transport of particles representing jellyfish in the LDB from their release to recapture. The passive movements of particles in water are influenced by several processes, including horizontal advection, horizontal dispersion, vertical advection, vertical dispersion, buoyancy and wind stress. As the vertical dispersion was less important comparing with the diel vertical migration of the jellyfish, it is not taken into consideration. Sensitive experiments show that the influence of directed wind drift on jellyfish movement is very small. Hence, the modeled jellyfish movement process includes the horizontal advection, the horizontal dispersion, and the DVM.

Influenced by light, the jellyfish always locate on the surface during the day and remain on the bottom of the sea at night (Berline et al., 2013). Because we could not locate information about the vertical migration speed of the jellyfish, we assume that it is the same as its horizontal speed. Jellyfish swim upward when the sun rises and begin to return downward at sunset. The sunrise and sunset time were calculated from the modeled date, latitude and time zone. As discussed above, jellyfish will move to the bottom or near-bottom of the LDB if they encounter strong winds (>5 m/s) during the day.

The passive movements of a particle can be determined as follows:

$$\frac{\mathrm{d}\vec{x}}{\mathrm{d}t} = \vec{u}_{\mathrm{p}} + u', \tag{1}$$

where $\vec{x}$ is the particle coordinate; $\vec{u}_{\mathrm{p}}$ is the drift velocity of particle at time t and position $\vec{x}$ which can be output from the OFS-C; and u' denotes the diffusion velocity. Once the initial position of a particle is assigned, its trajectory can be determined by solving Eq. (1). In this study, Eq. (1) was solved by the two-order Euler integration.

The diffusion velocity u' represents the sub-grid scale process that can not be solved by the circulation model under the model resolution. Generally, it is calculated by using a random walk technique, of which the sub-grid motion is treated as the random process. A simple random walk displacement velocities can be given by $R\sqrt{2r^{-1}K/\Delta t}$, which is known as the "naive walk" (Xue et al., 2008), where R random process with a expectation of 0 and standard deviation 1; and K is the horizontal diffusivity output from the ocean model, which is calculated using Smagorinsky (1963) scheme. Another commonly used formula is given by Visser (1997). This formula is more reliable in marine systems than the naïve walk, in which a turbulent diffusivity is commonly spatially non-uniform:

$$K'(x_n) + R\sqrt{2r^{-1}K(x_n + K'(x_n)\Delta t)/\Delta t}, \tag{2}$$

where $K'(x_n)$ represents the gradient of the diffusivity. On the basis of our sensitivity experiments for the LDB, no significant differences were observed between the two random schemes of the transport and distribution of jellyfish. Furthermore, the maps of the daily mean horizontal diffusivities in each layer of the LDB (not shown) are almost homogeneous, showing a consistent value of about 10 m^2/s (Fig. 3). Thus, water bodies with a homogeneous horizontal diffusivity field are not sensitive to the random walk method.

2.3 *Model simulations*

Jellyfish release spots should be located near breeding areas. There are five traditional release sites in the LDB (Fig. 1): the Xiaoling River Estuary in Jinzhou (JZ), the Lianshan Bay in Huludao (HLD), the Shuangtai River Estuary in Panjin (PJ), the Liaohe River Estuary in Yingkou (YK), and the Taiping Bay in Wafangdian (WFD) (Dong et al., 2013). The release spots used in our simulations were the actual release sites. Particles were randomly released into the water at a depth of 3–5 m, as the reported sites of actual jellyfish release (Dong et al., 2013). The fishing ground in the LDB is located at the northern part of the bay within the 5–10 m isobaths. At the time of release, the umbrella diameter of the jellyfish is approximately 1 cm, and they have nearly no swimming ability.

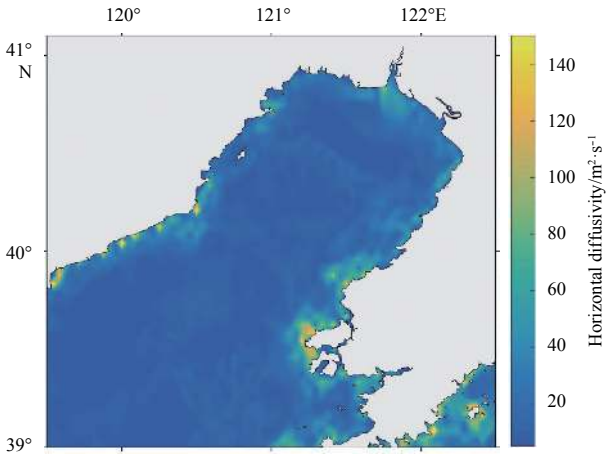

Fig. 3. Daily mean horizontal diffusivity on the sea surface on July 1, 2010.

The jellyfish population in the LDB is almost completely harvested during the fishing season. Usually, the fishing season occurs in July and lasts 2–3 d (Dong et al., 2009). Therefore, in the experiments of this study, particles were tracked for 2 months. The time interval for the particle tracking is 1 h. Since the temporal resolution of the forecast system output is 3 h, all the variables will be interpolated to 1 h using a linear interpolation of the particle tracking. The horizontal velocities were interpolated with a bilinear interpolation. In each experiment, 700 particles in total were released at each site, regardless of whether they were released in 1 d or over the course of several days.

To check the validation of the 3 h output of currents used in the tracking model, we implemented two experiments. In the first one, the particles were driven by the currents with time interval of 3 h; in the second one, the time interval is 1 h. In both the two experiments, the particles were released on the sea surface from five different sites and tracked for 50 d. The releasing time is at 12:00 o'clock on June 1, 2010. The results show that the trajectories of the particles in the two experiments are quite similar, which implies that 3 h output of the current is enough for the simulation (Fig. 4).

3 Results

3.1 *Model reliability*

A large-scale jellyfish stock enhancement was conducted by the Ocean and Fisheries Bureau of Liaoning Province from June 1 to June 7 in 2010. Afterwards, several surveys were carried out for the purposes of jellyfish research and management (Dong et al., 2013). The survey data were used to verify the reliability of the model. In this numerical experiment, 100 particles were released each day at noon from June 1 to June 7 at each site. Figure 5 shows the observed average product and simulated average jellyfish distribution from July 5 to July 13. In Fig. 5a, each dot denotes the average particle location which is simulated during the survey days. The main fishing ground is located in the northern region of the LDB at 40°30′N at depths of 5–10 m (Dong et al., 2009). The modeled distribution also indicates that the jellyfish mainly gather at the top of the bay within the 10 m isobaths and that a small proportion moves to the center of the bay, which is consistent with the survey. However, there are also several discrepancies between the simulation and the observation. These discrepancies may be attributed to the less of the jellyfish swim-

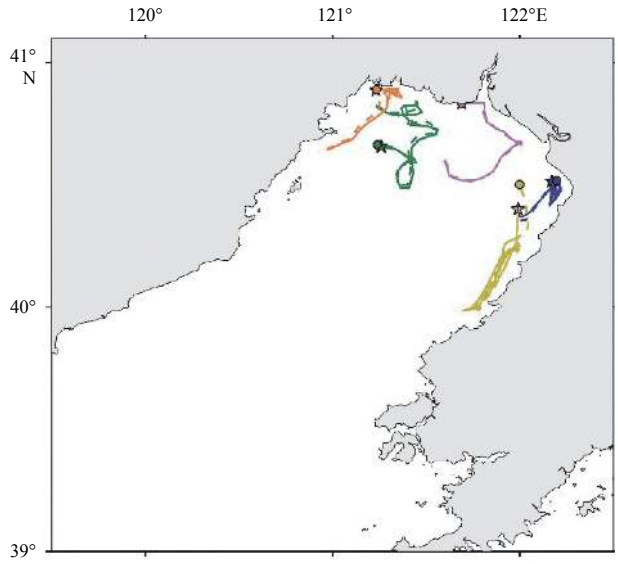

Fig. 4. Trajectory of particles simulated by the 3 h output current (dashed lines and cycles) and 1 h time interval current (solid lines and stars). Particles were released on the sea surface from five different sites. The releasing time is at 12:00 o'clock on June 1, 2010 and the tracking time is 50 d.

ming in the model.

3.2 *Distributions*

To investigate the characteristics of the jellyfish distribution and transport, we conducted three experiments for years 2008–2010. In these experiments, particles were released on June 1 of each year and tracked for about 2 months. The particle distributions after release on July 1 and July 20 (which is considered the general jellyfish fishing season) for the three modeled years are shown in Fig. 6.

The model runs generally reflected the features of the circulation in the LDB. Particles released at HLD and WFD tended to move northeast along the coast. Approximately 1 month later (July 1), most of the particles entered the shallow coastal waters within the 10 m isobaths. Particles at the top of the bay tended to move eastward. In 2010, particles in the area outside the 10 m isobaths were transported westward, into the center of the bay. The clockwise movement of the particles is consistent with the circulation pattern.

The jellyfish distribution patterns are influenced by the circulation structure of the LDB. Figure 7 shows the 2 months (June and July) average vertical mean current fields for each modeled year. Near the western coast of the LDB, the northeast current was strong and steady every year; thus, particles released at HLD were rapidly transported to the top of the bay. The current near the eastern coast (WFD) was relatively weak and unstable. In years when the westward component of the current was relative strong (such as 2010), particles released at WFD may move to the center of the bay (Fig. 6), which created adverse conditions for jellyfish harvesting.

The filled contours show the magnitude of the current. The arrows represent the direction of the flow.

Because the water depth is generally shallow in the LDB, the wind field can greatly affect the current structure and thereby the particle transport and distribution. Figure 8 shows the stick plot of the wind vectors averaged at the 10 m isobaths at the top of the bay for June and July. The corresponding vectors for the surface current are also shown. The direction and speed of the current are greatly impacted by the wind. In summer, the same as the wind, the current direction in the LDB is mainly northeastward and the velocity is consistent with those of the wind. Hence, the wind can indirectly influence the particles transport and distribution.

The distribution of jellyfish in the LDB is relatively stable and centralized, and interannual changes in their distribution are small, implying that the LDB is a suitable location for jellyfish stock enhancement. Overall, Figs 7–8 suggest that the particle distribution was significantly affected by both the currents and the wind. The southwest summer wind influenced the surface current, which drove the particles northeast along the coastline. The clockwise circulation carried the particles at the top of the bay to the east and those outside the 10 m isobaths to the west.

3.3 *Connectivity*

To optimize the release strategy, a connectivity matrix was constructed from the releasing sites to the fishing grounds for July 20, 2008–2010. The particles were released on June 1 of each year. As shown in Fig. 1, the areas with water depths of less than

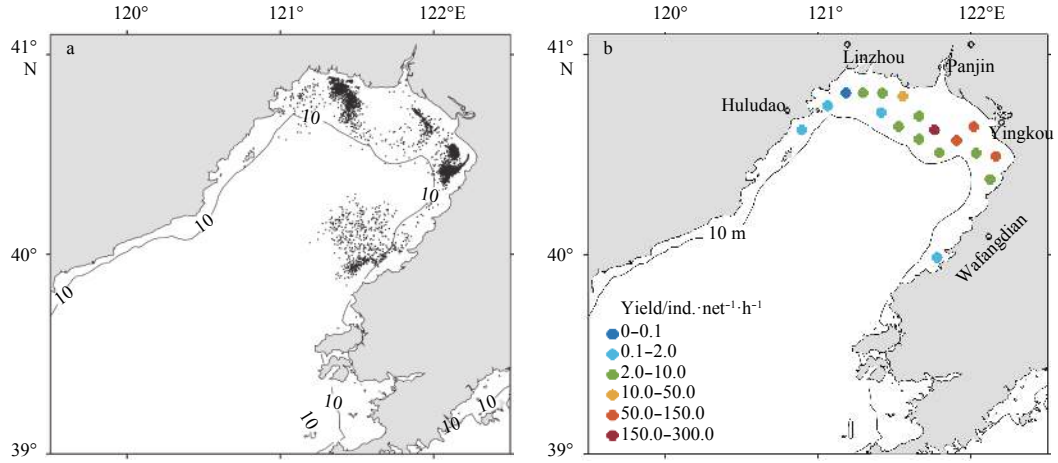

Fig. 5. Simulated mean distributions of jellyfish for July 5–13, 2010 (a) and observed mean hourly yields per net during the survey period for the same period (b) (redrawn from Dong et al., 2013). The dots represent the average particle location that is simulated during the survey days.

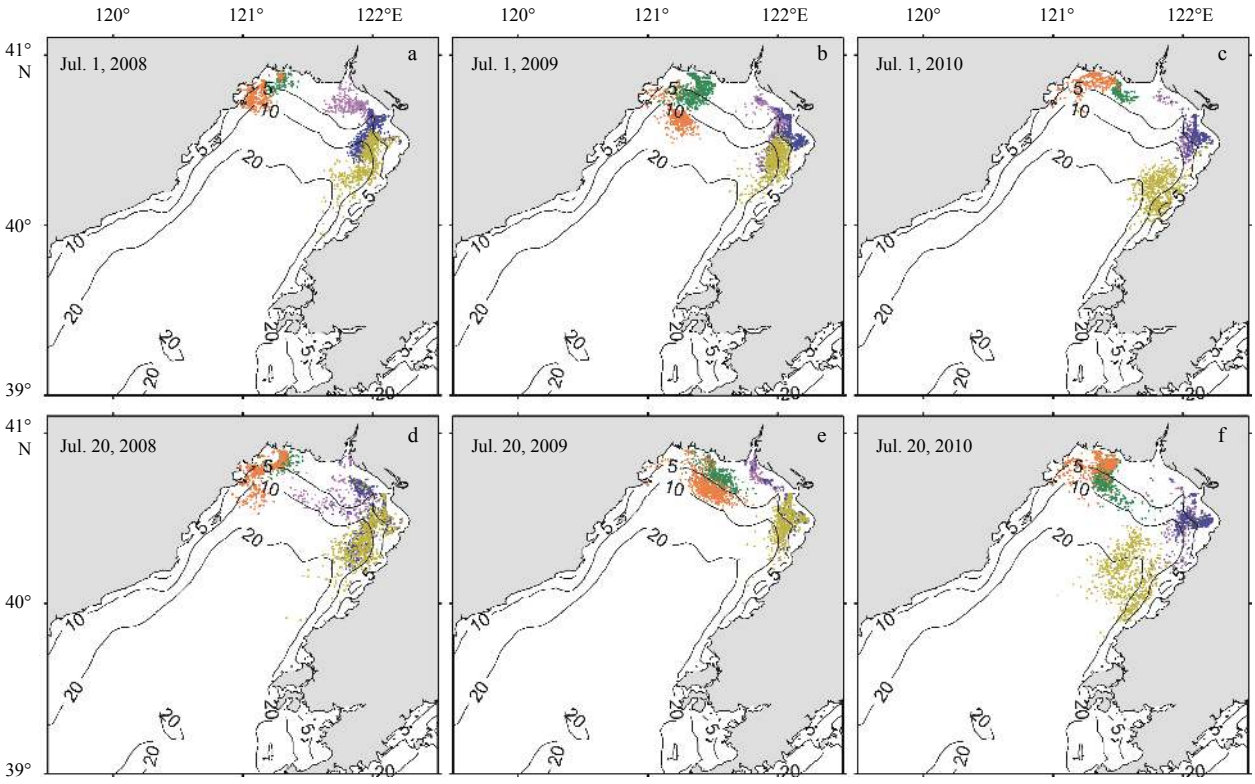

Fig. 6. Daily mean distributions of particles on July 1 (upper panel) and July 20 (lower panel) of 2008–2010. Particles were released on June 1 at the sites shown in Fig. 1: HLD (orange), JZ (green), PJ (magenta), YK (blue), and WFD (yellow).

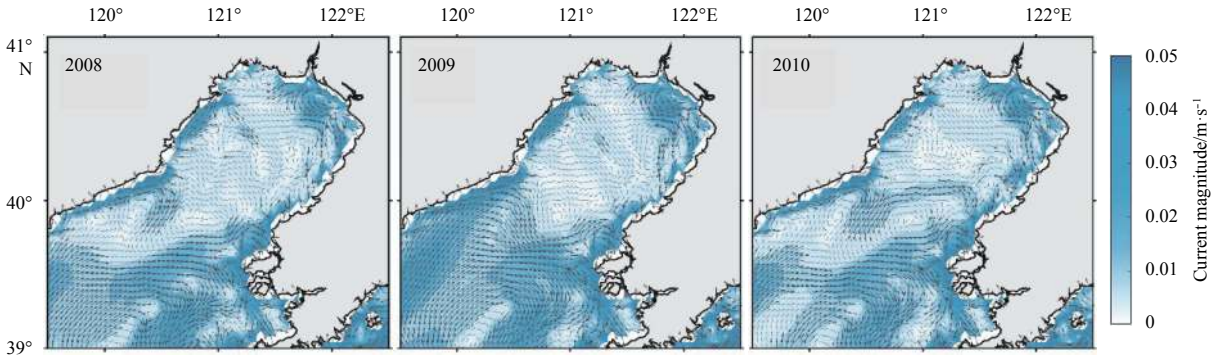

Fig. 7. Vertically average current during June and July in 2008, 2009 and 2010.

10 m (traditional fishing grounds) were divided into five regions according to their administrative divisions. In the matrix, values X_{ij} was calculated as the percentage of the particles released from Site j (y-axis in Fig. 9) that were transported to fishing area C_j at a specific time (x-axis in Fig. 9). After 50 d of integration, only a small part of the particles released from HLD retained at the fishing ground C1, while most of them had moved to the fishing ground C2 and some can reach at C3. The particles released at JZ, PJ and YK remained at the fishing ground closest to their release sites (C2 to C4), and the remainders were transported to a neighboring fishing ground. Most of the particles released at WFD were transported to C4, while some moved out of the fishing grounds.

The summation of Row j represents the percentage of particles released from Site j that are transported to any of the five fishing grounds (hereafter referred to as the retention rate). A retention rate of 1 indicates that all of the particles are transported to the fishing grounds (Table 1). Almost all of the particles released from HLD, JZ, PJ and YK are transported to the fishing ground in each of the three modeled years. This implies that the jellyfish released from these sites are highly likely to be caught during the fishing season. However, the particles released from WFD exhibited retention rates of only 0.45 and 0.27 in 2008 and 2010.

Summation of column i yields the amount of particles that were transported to fishing ground i from all five release sites (Table 2). A higher value implies a better fishing ground. The majority of particles accumulated at C2, C3 and C4. A very small proportion of the particles were transported to C1 and C5, indicating that C2 through C4 are the most abundant fishing grounds.

3.4 *Lagrangian probability density function*

To further assess the distribution of the jellyfish in the fishing

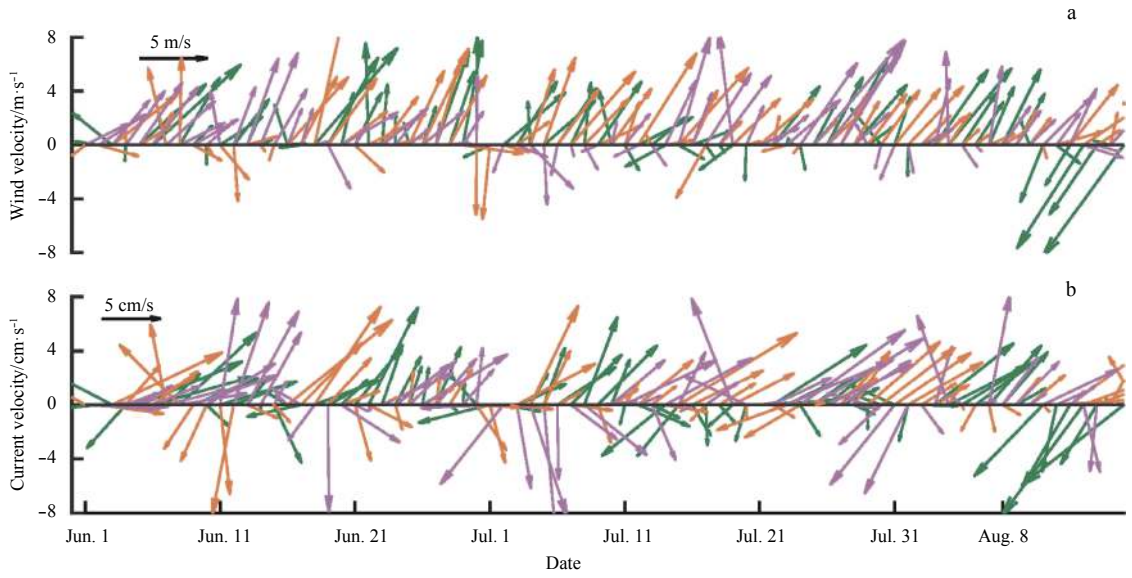

Fig. 8. Stick plot of the daily mean wind (a) and surface current (b) vectors for June and July of 2008 (green), 2009 (orange), and 2010 (magenta). Values are the average at the 10 m isobath at the top of the bay (Regions C2 through C4, Fig. 1).

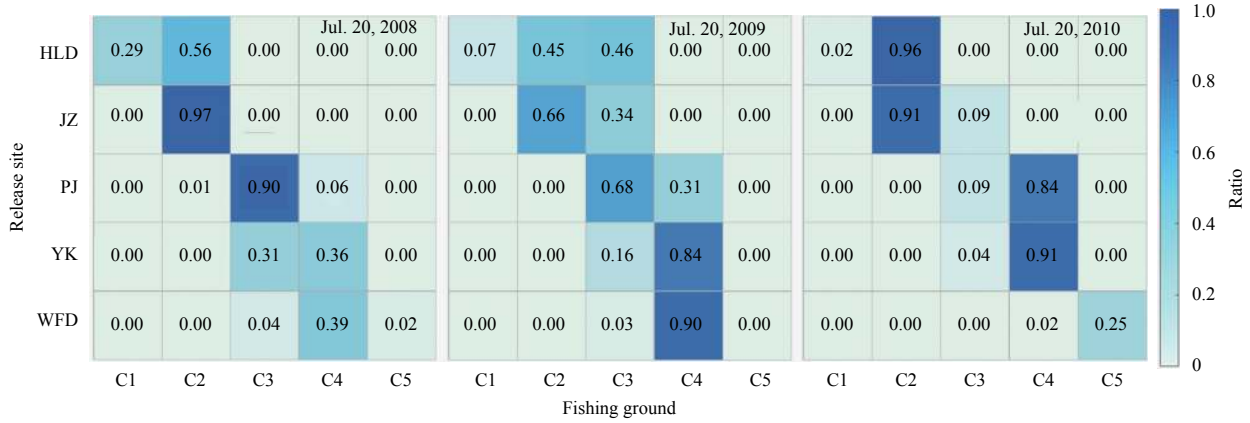

Fig. 9. Connectivity matrixes of the particles from the release sites to the fishing grounds (Fig. 1) on June 20, 2008–2010. Values in the matrix are the ratios of particles that arrived at a fishing ground (x-axis) to the particles released at a given release site (y-axis).

Table 1. Row summation of the connectivity matrix shown in Fig. 9 for 2008–2010

Year	HLD	JZ	PJ	YK	WFD
2008	0.85	0.97	0.98	0.67	0.45
2009	0.98	1.00	0.99	1.00	0.93
2010	0.98	0.99	0.93	0.95	0.27

Table 2. Column summation of the connectivity matrix shown in Fig. 9 for 2008–2010

Year	C1	C2	C3	C4	C5
2008	0.30	1.54	1.25	0.81	0.02
2009	0.07	1.11	1.66	2.05	0.00
2010	0.02	1.86	0.22	1.76	0.25

grounds and the expected dispersal patterns of jellyfish released from each site, the Lagrangian probability-density functions (PDFs) (Mitarai et al., 2009) based on a 9 a tracing experiment were used. The PDFs represent the expected locations of particles released from a specific site at a given advection time τ and can be derived by a Gaussian filter from a discrete Lagrangian PDF; this derivation is expressed as follows:

$$f_X(\xi;\tau,a) \approx \frac{1}{\pi R^2}\int_{|r|\leqslant R} f'(\xi;\tau,a+r)\mathrm{d}r, \tag{3}$$

where R is the radius of each site; ξ is the sample space variable for X; and $f_X{}'$ is the discrete representation of the Lagrangian PDFs.

$$f_X{}'(\xi;\tau,a) = \frac{1}{N}\sum\left[\delta X_n(\tau,a)-\xi\right], \tag{4}$$

where N is the total number of particles released at the given site and δ is Dirac delta function.

To obtain the PDFs, a sufficient quantity of variable samples was needed. As the release time for jellyfish enhancement is from late May to early June every year from 2008 through 2016, 100 particles were released at 06:00 am and 12:00 am each day from May 16 through June 15 at each site; in total, 31 000 particles were

released from the five stations in the experiment. The growth time of jellyfish for enhancement in the LDB is approximately 50 d every year, so the Lagrangian PDFs from the five sites at 50 d after their release was calculated (Fig. 10).

The majority of the jellyfish released from Sites HLD, JZ, PJ and YK accumulated within the 10 m isobath (Figs 10a–d), which is favorable for jellyfish fishing. However, the jellyfish released from WFD may have the probability entering into the center of the bay, some can leave the bay carried by the clockwise current (Fig. 10e). This confirms the results of the connectivity matrix. Figure 10 illustrates that for the whole jellyfish released from all the five sites, the probability that the jellyfish arrive at the northeast of the bay is larger than that at the northwest of the bay, which is consistent with the observation (Dong et al., 2013). Generally, the Lagrangian PDFs provide a "climatology" vision of the distribution for the releasing jellyfish in the LDB.

3.5 *Sensitivity analysis*

Several numerical experiments were conducted to investigate the sensitivity of the simulated distributions to the algorithm and the release conditions used. Simulations were repeated without a random walk and with different random walk schemes, habitat depths, and release dates. Details of the model designs are shown in Table 3.

3.5.1 *Random walk*

To investigate the effects of different random walk schemes on the particle distribution and the sensitivity of the model to the random walk scheme, several different random walk schemes were tested. In these experiments, the particles were released on June 1, and their locations were recorded on July 20. Figure 11a shows the distribution of the particles without incorporating a random walk into the model. In this case, the horizontal transport driven by only the current determined the trajectories of jellyfish. However, the particles clustered extensively without a random walk.

By introducing a random walk, the aggregation caused by the lack of subgrid scale processes was significantly reduced, and the scope of the distribution was significantly increased. Figures 11b–d show the particle distributions after incorporating three random walk schemes into the model: a naive walk with a fixed horizontal diffusivity of 20 m^2/s, a naive walk with the realistic horizontal diffusivity calculated from the ocean model, and Visser's scheme (Table 3). The results of the random walk experiments were similar, implying that the trajectories were insensitive to the random scheme and that the particle-tracking algorithm used in our study is robust.

3.5.2 *Habitat depth*

The horizontal flow in the LDB is affected by the surface wind and the bottom topography. Therefore, the flow speeds change rapidly from the upper layer to the bottom and even the direction of circulation in the bottom layer may be opposite to that in the upper layer (Fig. 12). On the surface, the current is heavily in-

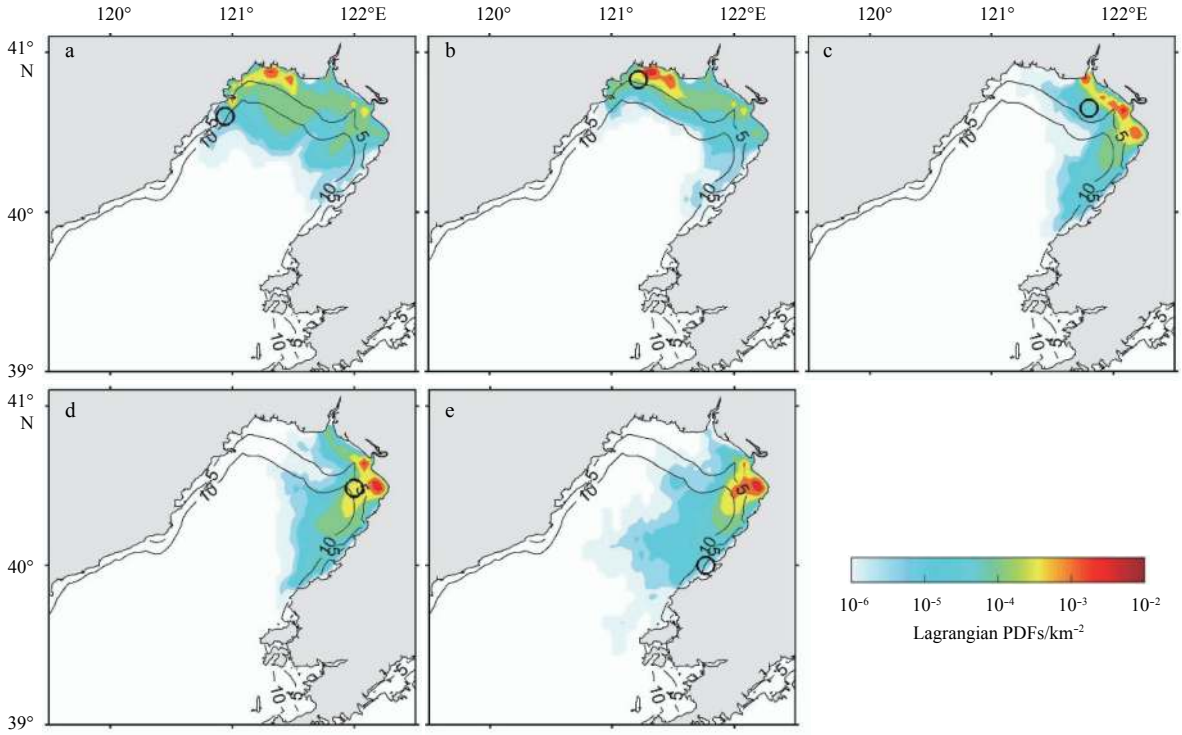

Fig. 10. Lagrangian PDFs from the five sites for an advection time of 50 d. Figures 10a–e show the results for the five source sites (HLD, JZ, PJ, YK and WFD, respectively). Source sites are marked with the black circles.

Table 3. List of numerical sensitivity experiments

Run	DVM	Random walk scheme	Release depth/m	Release date
R1	on	off, simple walk with K=20; simple walk with realistic K, Visser	4	Jun. 1, 2010
R2	off	Visser	0.1, 1, 4	Jun. 1, 2010
R3	on	Visser	4	May 25, Jun. 1, Jun. 7, 2010

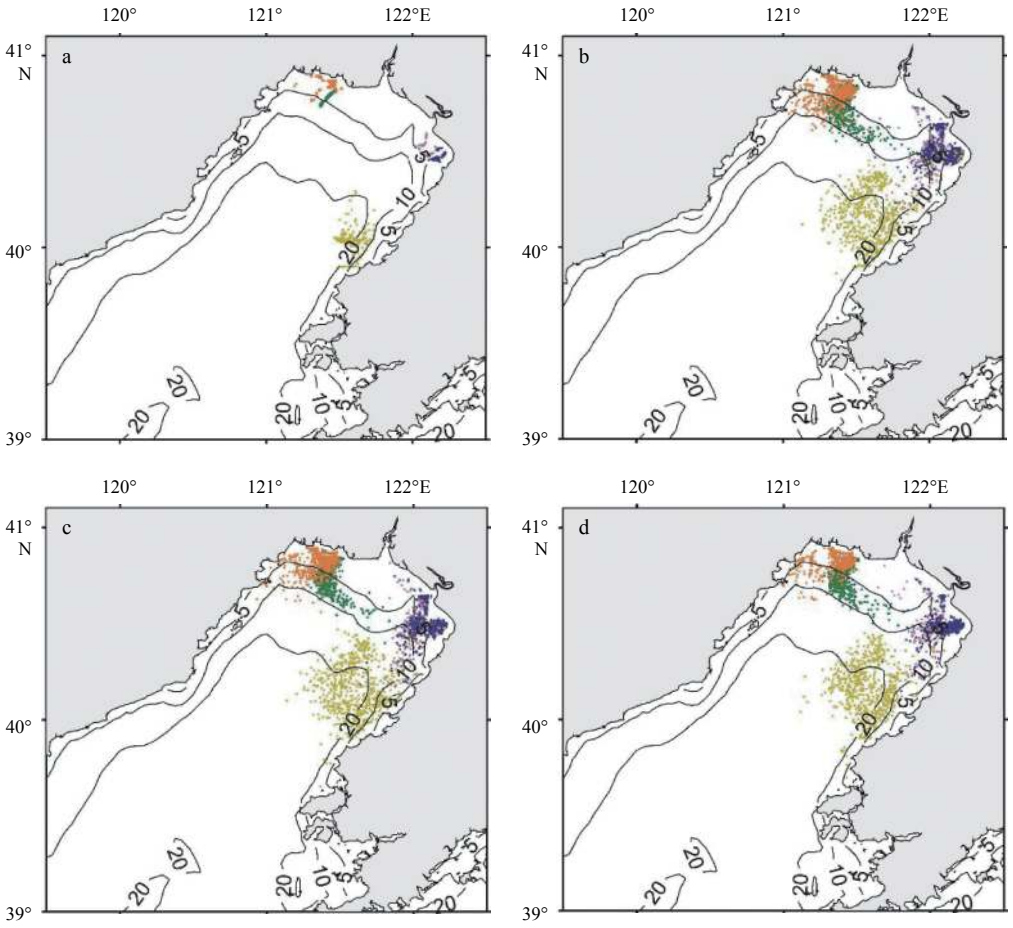

Fig. 11. Distribution of particles on July 20 after release on June 1, modeled with no random walk (a), a naive walk with a fixed horizontal diffusivity of K=20 m^2/s (b), a naive walk with a realistic K value from the hydrodynamic model (c) and Visser's scheme (d). Colors distinguish the particles released at different sites shown in Fig. 1: HLD (orange), JZ (green), PJ (magenta), YK (blue), and WFD (yellow).

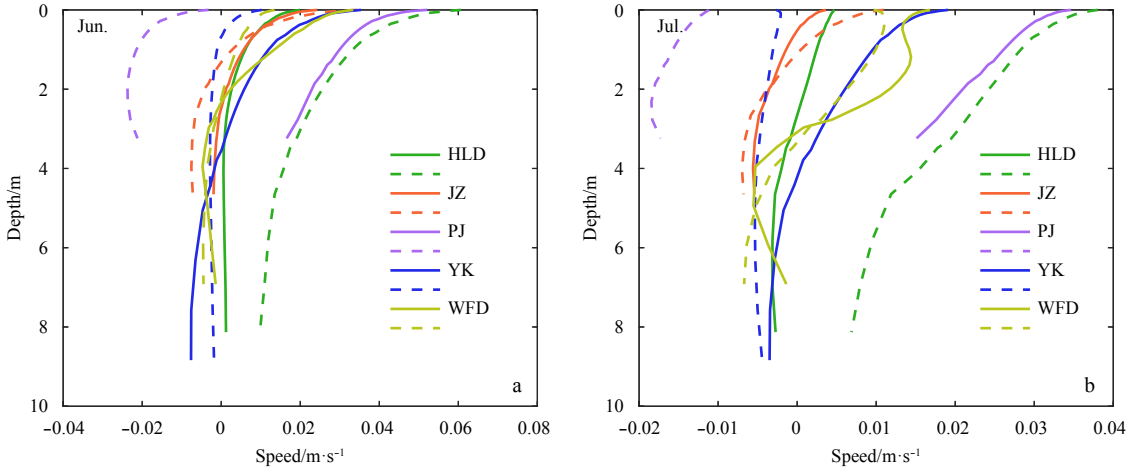

Fig. 12. Vertical structures of the monthly mean current at the five release sites shown in Fig. 1 in June (a) and July (b) of 2010. The solid and dashed lines represent the current speeds u and v, respectively.

fluenced by the wind, and the direction is similar to that of the wind (Fig. 8). In the bottom layer, the current speed is significantly lower, and clockwise circulation can be observed (Fig. 2). Thus, particle trajectories may differ significantly within different water layers.

Figure 13 shows the distributions of particles on July 20 after being released in three different layers on June 1, 2010. In these experiments, vertical migration was excluded, and the particles were fixed at depths of 0.1, 1 or 4 m. The particles in the surface layer were driven by the surface current, which was dominated

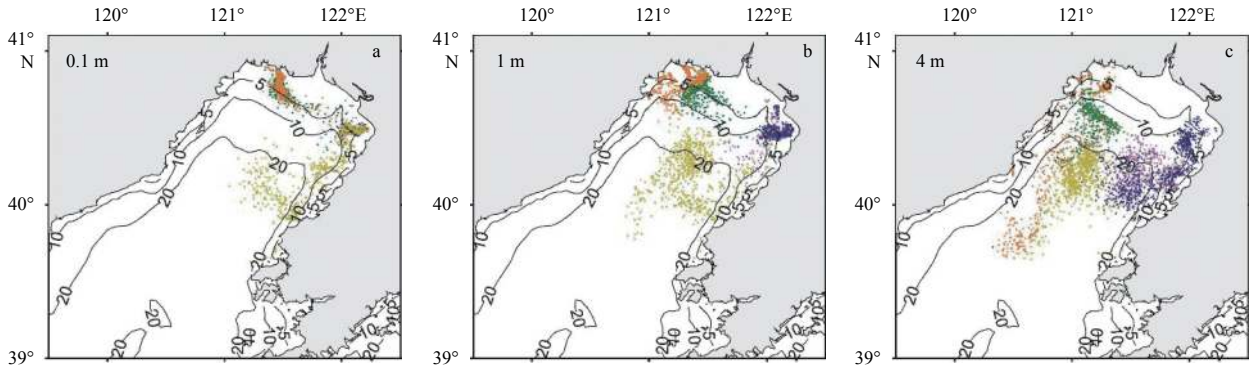

Fig. 13. Distribution of particles which maintained at fixed depths of 0.1 m (a), 1 m (b), or 4 m (c) on July 20 after release on June 1, which indicates the great impact of jellyfish depth on their horizontal distribution. Colors distinguish the particles released at different sites shown in Fig. 1: HLD (orange), JZ (green), PJ (magenta), YK (blue), and WFD (yellow).

by the summer wind. These particles were transported northeast towards the top of the bay and eventually concentrated along the northern coastline. The particles at deeper depths were less influenced by the wind. The transport of particles at the lowest modeled depth (4 m) was dominated by the bottom circulation, which resulted in the particles being distributed across most of the bay and into the bay mouth. Thus, it is anticipated that the jellyfish could remain on the sea surface longer than on the bottom, which will be propitious for their aggregation at the bay top and for jellyfish recapture.

3.5.3 *Release date*

In this group of sensitivity experiments, the particles were released on May 25, June 1, June 8 or June 15 to examine the influence of the release date on the distribution of jellyfish. The general distribution patterns for the four release dates were similar (Fig. 14). However, some differences were observed from the results of the experiments. For instance, for the jellyfish released at

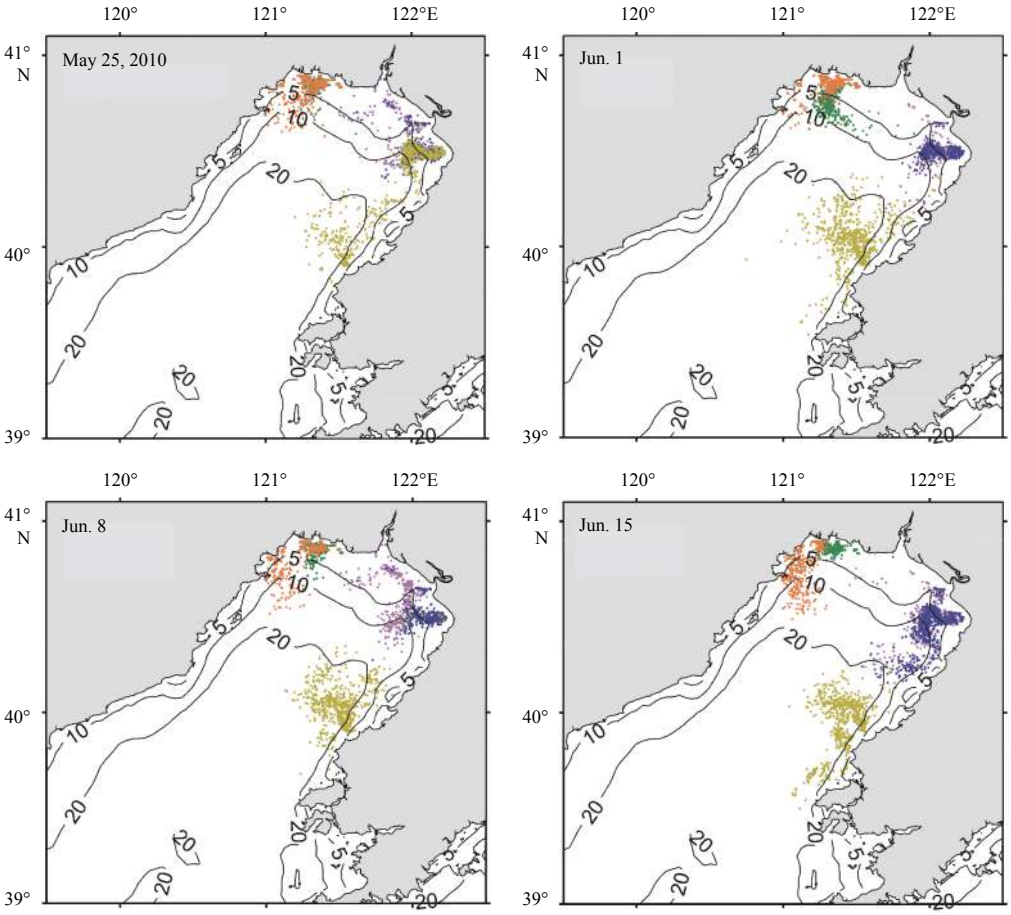

Fig. 14. Distribution of particles on July 20 after release on May 25, June 1, June 8 and June 15. The particles were released at the sites shown in Fig. 1: HLD (orange), JZ (green), PJ (magenta), YK (blue), and WFD (yellow).

WFD, those released earlier were more likely to be transported to the fishing ground than those released later; previously, we found that the jellyfish released at WFD were the least likely to enter the fishing area (Table 1). Furthermore, under the continuous influence of the southwest summer wind, the jellyfish that remained in the sea longer were transported closer to the northern coastline of the bay. As shown in Fig. 14, most of the particles released on May 25 arrived at the northern coast of the bay, while the particles released on June 15, especially those released at WFD, were located far from the northern coast. Thus, if other environmental conditions, such as the temperature and sufficient food, are suitable for jellyfish release, we suggest that the jellyfish should be released as early as possible to improve the retention rate. Of course, earlier releases mean that the jellyfish face lower water temperature and less food, which may result in their death. Therefore, the balance between early release and having appropriate sea water temperature and sufficient food is crucial.

4 Discussion and conclusions

In this study, the jellyfish trajectories were calculated using the Lagrangian particle tracking method with current and horizontal diffusivity values obtained from the OFS-C. Sensitivity numerical experiments demonstrates that the algorithm is robust to different random walk schemes. The simulated distribution patterns show qualitative agreement with the survey results from 2010 (Fig. 5). The simulation results and the observations both indicate that most of the jellyfish accumulate at the top of the bay within the 10 m isobaths, with a small proportion being transported to the eastern and western coasts and even to the center of the bay. In addition, the 3 a simulation from 2008 to 2010 shows that although there are several distinctions between the distributions in different years, the general patterns are similar, and the majority of the jellyfish will gradually move to the top of the bay after their release. Overall, the results imply that the shallow northern region of the LDB is a favorable fishing ground, which is in accordance with previous hypothesis (Dong et al., 2009).

The current and the wind are the main factors that impact the transport of jellyfish in the LDB. As the annual change in the bottom circulation in the LDB is not obvious, the yearly variation in jellyfish transport is mainly caused by the surface current, which is strongly influenced by the wind. In the years in which the southwest wind is sustained, the northeast surface current is correspondingly intensified. As a result of DVM, jellyfish spend the day on the sea surface and will be carried to the north end of the bay.

Connectivity matrices for the transport simulations indicate that most of the released jellyfish accumulate at the anticipated fishing regions during the fishing season. Approximately two months after release, the jellyfish released at JZ, PJ and YK will strand at the corresponding fishing grounds C2 to C4 (Fig. 1), while those released at HLD will travel northward and into the C2 fishing ground. The distribution of jellyfish released at WFD was found to vary significantly: jellyfish were transported into the fishing ground C4 in some years (such as 2008 and 2009) but were transported away from the fishing area in 2010. Hence, HLD, JZ, PJ and YK are appropriate release sites, and C2, C3 and C4 are the optimal fishing grounds.

To further verify the matrix results, the Lagrangian PDFs, which were derived based on a 9 a particle tracking (2008–2016) during late May through early June, for 50 d after release from the five sites was calculated, . The PDFs clearly exhibit the probability that the particle released from a specific site can arrive at the study area. In addition, the PDFs validated the connectivity matrix results.

The study shows that if the jellyfish always inhabited the bottom of the bay, they would be transported out of the bay by the bottom circulation, especially that released from WFD. Particles released on different dates showed that due to the continuous effect of the summer wind, the particles that stayed in the water longer were transported closer to the northern coastline of the bay. Thus, if the environmental and ecological conditions are suitable, it is recommended that jellyfish can be released as early as possible to optimize the retention rate.

The model could explain the general distribution patterns of the releasing jellyfish, but there were still deviations between the simulated results and the observations. It can be observed from the survey results (Fig. 5a) that the maximum catch occurs at the center of the bay top, while the simulation (Fig. 5b) shows that most of the jellyfish accumulate on the eastern and western sides of the bay top. This discrepancy may be attributed to the exclusion of biological processes and ecological factors from the model. In fact, the salinity, amount of precipitation, food supply, and jellyfish swimming and assemblage characteristics can also influence the distribution and survey results of the jellyfish. In the future study, we will establish an individual-based model that incorporates the growth and mortality of the jellyfish to refine the simulation and further investigate the factors that influence the recapture rate.

References

Berline L, Zakardjian B, Molcard A, et al. 2013. Modeling jellyfish *Pelagia noctiluca* transport and stranding in the Ligurian Sea. Marine Pollution Bulletin, 70(1–2): 90–99

Dong Jing, Jiang Lianxin, Tan Kefei, et al. 2009. Stock enhancement of the edible jellyfish (*Rhopilema esculentum* Kishinouye) in Liaodong Bay, China: a review. Hydrobiologia, 616(1): 113–118

Dong Jing, Jiang Lianxin, Sun Ming, et al. 2013. Biological Research on Large Jellyfish in Bohai Sea and North of Huanghai Sea (in Chinese). Beijing: China Ocean Press, 49-57

Grimm V. 1999. Ten years of individual-based modelling in ecology: what have we learned and what could we learn in the future? Ecological Modelling, 115(2–3): 129–148

Jiang Wensheng, Wu Dexing, Gao Huiwang. 2002. The observation and simulation of bottom circulation in the Bohai Sea in summer. Journal of Ocean University of Qingdao (in Chinese), 32(4): 511–518

Jin Xianshi. 2014. Foundation and Prospect of Stocking Enhancement for Fishery Resources in Huanghai and Bohai Sea (in Chinese). Beijing: Science Press, 235-236

Li Guojiang, Ti Jianxin, Chen Rongjie. 2008. Discussion of measures to increase the recapture rate of edible jellyfish. Shandong Fisheries (in Chinese), 25(12): 51–52

Mitarai S, Siegel D A, Watson J R, et al. 2009. Quantifying connectivity in the coastal ocean with application to the Southern California Bight. Journal of Geophysical Research: Oceans, 114(C10): C10026, doi: 10.1029/2008JC005166

Moon J H, Pang I C, Yang J Y, et al. 2010. Behavior of the giant jellyfish *Nemopilema nomurai* in the East China Sea and East/Japan Sea during the summer of 2005: a numerical model approach using a particle-tracking experiment. Journal of Marine Systems, 80(1–2): 101–114

Omori M, Nakano E. 2001. Jellyfish fisheries in Southeast Asia. Hydrobiologia, 451(1–3): 19–26

Pitt K A, Kingsford M J. 2003. Temporal variation in the virgin biomass of the edible jellyfish, *Catostylus mosaicus* (Scyphozoa, Rhizostomeae). Fisheries Research, 63(3): 303–313

Qiao Fangli. 2012. Chinese Regional Oceanography-Physical Oceanography (in Chinese). Beijing: China Ocean Press, 25-26

Qiao Fangli, Ma Jian, Yang Yongzeng, et al. 2004a. Simulation of the temperature and salinity along 36°N in the Yellow Sea with a

wave-current coupled model. Journal of the Korean Society of Oceanography, 39(1): 35–45

Qiao Fangli, Xia Changshui, Shi Jianwei, et al. 2004b. Seasonal variability of thermocline in the Yellow Sea. Chinese Journal of Oceanology and Limnology, 22(3): 299–305

Smagorinsky J. 1963. General circulation experiments with the primitive equations. Monthly Weather Review, 91(3): 99–164

Visser A W. 1997. Using random walk models to simulate the vertical distribution of particles in a turbulent water column. Marine Ecology Progress Series, 158: 275–281

Wang Guansuo, Zhao Chang, Xu Jiangling, et al. 2016. Verification of an operational ocean circulation-surface wave coupled forecasting system for the China's seas. Acta Oceanologica Sinica, 35(2): 19–28

Xia Changshui, Qiao Fangli, Zhang Mengning, et al. 2004a. Simulation of double cold cores of the 35°N section in the Yellow Sea with a wave-tide-circulation coupled model. Chinese Journal of Oceanology and Limnology, 22(3): 292–298

Xia Changshui, Qiao Fangli, Zhang Qinghua, et al. 2004b. Numerical modelling of the quasi-global ocean circulation based on POM. Journal of Hydrodynamics, 16(5): 537–543

Xiong Xuejun, et al. 2012. China Offshore Oceanography-Marine Meteorology and Physical Oceanography (in Chinese). Beijing: China Ocean Press, 210-212

Xue Huijie, Incze L, Xu Danya, et al. 2008. Connectivity of lobster populations in the coastal Gulf of Maine: Part I. Circulation and larval transport potential. Ecological Modelling, 210(1-2): 193–211

Yang Yongzeng, Qiao Fangli, Zhao Wei, et al. 2005. MASNUM ocean wave numerical model in spherical coordinates and its application. Haiyang Xuebao (in Chinese), 27(2): 1–7

You Kui, Ma Caihua, Gao Huiwang, et al. 2007. Research on the jellyfish (*Rhopilema esculentum* Kishinouye) and associated aquaculture techniques in China: current status. Aquaculture International, 15(6): 479–488

Yuan Yeli, Hua Feng, Pan Zengdi, et al. 1991. LAGDF-WAM numerical wave model-I. Basic physical model. Acta Oceanologica Sinica, 10(4): 483–488

Zhao Baoren, Zhuang Guowen, Cao Deming, et al. 1995. Circulation, tidal residual currents and their effects on the sedimentations in the Bohai Sea. Oceanologia et Limnologia Sinica (in Chinese), 26(5): 466–473